REGISTRATION OF VLF-SFERICS AT THE VON-NEUMAYER STATION

H. VOLLAND[1], M. SCHMOLDERS[1], G. PRÖLSS[2] and H. KRÖNINGER[3]

[1]*Radioastronomisches Institut, Universität Bonn, 5330 Bonn-Enderich, Auf dem Hügel 71, German Federal Republic*
[2]*Institut für theoretische Astrophysik, Universität Bonn, 5330 Bonn-Enderich, Auf dem Hügel 71, German Federal Republic*
[3]*National Electrical Engineering Research Institute, Pretoria, South Africa*

Abstract: A VLF-sferics-analyzer was operating at the German antarctic station von-Neumayer from January to July 1983. This analyzer registrated far distant lightning events in the frequency range between 5 and 9 kHz. Assuming the location of these sources to be known, the propagation characteristics of the atmospheric wave guide between the earth and the ionosphere can be derived along the propagation path. The method of measurement is described. The data of June 1983 are evaluated and the distances of the sources are determined from a comparison with rain fall records during the same month and, in addition, from sferics registrations obtained at a second station in Pretoria, South Africa. The main result is that the ionospheric *D* layer along the propagation paths from the east coast of South America to the von-Neumayer station and from South Africa to the von-Neumayer station do not show a significant daily variation. The virtual ionospheric reflection height is about 82 km for VLF waves between 5 and 9 kHz during June. This corresponds to night time conditions at northern mid-latitudes in winter.

1. Introduction

Sferics are electromagnetic pulses generated by lightning strokes. The very low frequency component (VLF; 3 to 30 kHz) of sferics can propagate in the atmospheric wave guide between the earth and the ionospheric *D* layer. The virtual ionospheric reflection height of VLF waves is about 70 km during the day and about 80 km during night time conditions.

Lightning strokes are powerful transmitters of VLF pulses. These signals become only weakly attenuated in the atmospheric wave guide and can travel large distances (several 1000 km) before these amplitudes fall below the noise level of the receiver. The atmospheric wave guide is dispersive and modulates the wave form of a sferic during its propagation. In principle, a determination of the wave form and of the direction of arrival for an individual sferic is therefore sufficient to determine the location of the lightning stroke. Several methods exist to locate thunderstorm areas via measurements in the VLF range (VOLLAND, 1982).

VLF sferics measurements are made either to determine the source properties (*e.g.*, the characteristics of the lightning strokes and their spatial distribution) or to determine the wave guide characteristics (*e.g.*, temporal and spatial variations of the propagation conditions). Both objects are intimately related to each other. In order to study the source properties, one has to know the wave guide characteristics, and vice versa. A third goal of VLF sferics observations is the determination of the natural radio noise level which limits long range radio communication (SPAULDING, 1982).

In this paper, we determine the propagation characteristics of the atmospheric wave guide from VLF sferics measurements obtained at Pretoria, South Africa, and at the von-Neumayer station, Antarctica, during June 1983. The frequency range is 5 to 9 kHz. No commercial transmitter is operating in this frequency range, and the Siple station, Antarctica, has presently discontinued its operation.

2. Method of Measurement

In this section, a brief description of the method of measurement is given. Further details about the instrument and the method of analysis can be found in VOLLAND *et al.* (1983).

Sferics originating more than several hundred km away from the receiver are mainly electromagnetic pulses generated by the vertically orientated section of lightning channels of return strokes. These pulses behave to a first approximation like the radiation component of a vertical electric dipole located on well conducting ground. The electromagnetic far-field component of such pulses consists of a vertical electric field E_z and of a horizontal magnetic field B_ϕ transverse to the direction of propagation. The magnetic field is used to determine the angle of arrival ϕ applying the well-known direction finding method based on two crossed loop antennas and a whip antenna.

The vertical electric field component of each sferic is Fourier analyzed by means of three narrow band receivers at 5, 7 and 9 kHz. The resultant spectral function $E_z(f, \rho)=|E_z(f, \rho)| \exp[i\theta(f, \rho)]$ is the product of the spectral source function $G(f)=|G(f)| \exp[i\xi(f)]$ and of the transmission function $W(f, \rho)=|W(f, \rho)| \exp[i\Psi(f, \rho)]$ of the atmospheric wave guide:

$$E_z(f, \rho)=G(f)W(f, \rho)=|G|\,|W| \exp[i(\xi+\Psi)]=|E_z| \exp[i\theta]\ . \tag{1}$$

Apart from the frequency f, the transmission function W depends on the distance ρ between source and receiver. It depends, in addition, on the direction of arrival ϕ (HARTH, 1982). The spectral function depends on frequency, on the electrical moment of the lightning stroke and on channel parameters such as channel length and diameter.

For each received sferic, the following parameters are determined:

(a) Spectral amplitude

$$\mathrm{SA}=20 \log |E_z(f_0)|\ , \tag{2}$$

(b) Spectral amplitude ratio

$$\mathrm{SAR}=20 \log \frac{|E_z(f_2)|}{|E_z(f_1)|}\ , \tag{3}$$

(c) Group time delay difference

$$\mathrm{GDD} = \frac{[\theta(f_1)+\theta(f_2)-\theta(f_0)]}{2\pi(f_0-f_1)}\,, \tag{4}$$

(d) Angle of arrival ϕ.
Here, $f_1=5$ kHz, $f_2=9$ kHz, and $f_0=7$ kHz.

Each parameter set (SA, SAR, GDD, ϕ) is stored in a desk top computer HP 9825 during a measurement cycle of 20 min. Figure 1 shows the observed GDD-values *vs.* azimuth angle ϕ for a time interval of 18 min between 1940 and 2000 GMT on August 20, 1984, observed in Bonn. Five clusters of points are evident which can be attributed to five thunderstorm areas. Figure 2 shows the corresponding SAR-data *vs.* azimuth during the same time interval, where the same thunderstorm areas can be identified. From a histogram of the numbers of GDD- (or SAR-) events *vs.* azimuth (Fig. 3, lower panel), one can find the azimuth of the centers of the thunderstorm areas with an accuracy of about one degree. For each source, similar histograms are also generated for the GDD, SAR, and SA data. As an example, the upper panel in Fig. 3 presents the respective histograms for the most intensive source at an azimuth of 104° (which is east-south-east of Bonn). A Gaussian fit to these histograms yields statistical mean values of the parameters, *i.e.*, $\overline{\mathrm{GDD}}$, $\overline{\mathrm{SAR}}$, $\overline{\mathrm{SA}}$, and $\overline{\phi}$. As discussed in the next section, these quantities are the basic information needed to determine the distance of the source. The data processing is completed in two minutes. In a final step, the four relevant source parameters and some source identifiers are stored on magnetic tape.

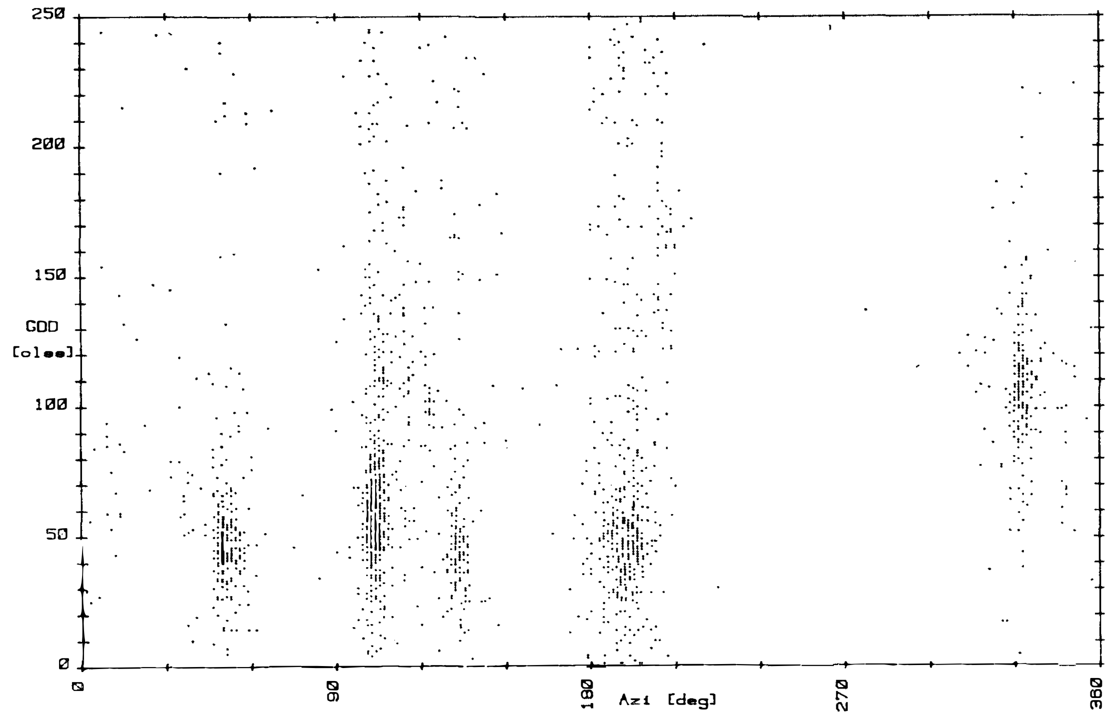

Fig. 1. GDD-values vs. azimuth observed during the time interval 1940 to 2000 GMT on August 20, 1984, at Bonn. Each point corresponds to one or more sferic signals. The azimuth (or direction of arrival) is counted in clockwise direction from geographic north. The units of GDD are arbitrary.

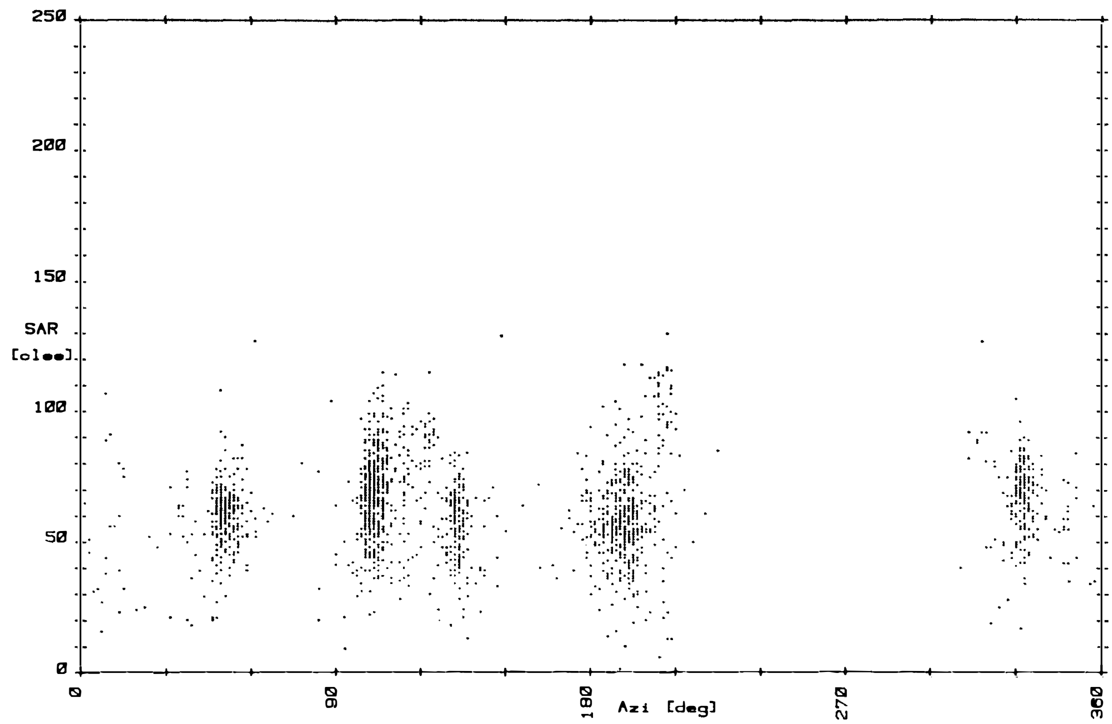

Fig. 2. SAR-values vs. azimuth. Otherwise the same as in Fig. 1.

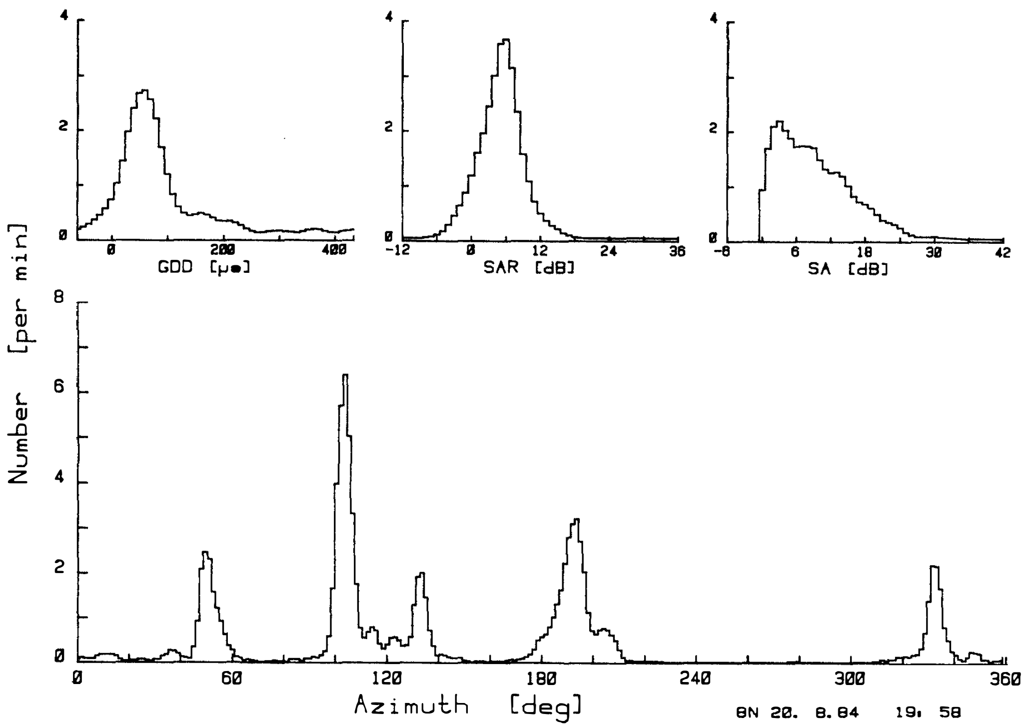

Fig. 3. Histogram of all recorded GDD-values as function of azimuth for the time interval indicated in Fig. 1 (lower panel); and histograms of the spectral parameters GDD, SAR and SA for the strongest source at 104° azimuth (upper panel).

The location of the thunderstorm centers can be plotted on a map in real time. An observer can thus study the actual thunderstorm activity in the wider surroundings of the station. One magnetic tape cassette can store the data of about three to four weeks.

3. Data Evaluation

In this section, we discuss how the distance of the source is determined from the mean values $\overline{\text{GDD}}$ and $\overline{\text{SAR}}$. The theory of VLF propagation within the atmospheric wave guide predicts a transmission function W at larger distances ($\rho > 1000$ km) of the form

$$W(f, \rho) = C(\rho/f)^{1/2} \exp[(-A+iB)\rho] , \tag{5}$$

where A is an attenuation factor and B is a propagation factor, both depending on frequency, angle of arrival, local time and season (*e.g.*, HARTH, 1982). C is a constant factor.

The spectral source function G can be approximated by that of a vertical electric dipole. If the electric current of this dipole has a temporal variation of the general form

$$J = J_0[\exp(-\alpha t) - \exp(-\beta t)] , \tag{6}$$

then the spectal function is given by

$$G = -\frac{i\omega M\alpha\beta\mu}{4\pi\rho(\alpha-i\omega)(\beta-i\omega)} , \tag{7}$$

where $\mu = 4\times 10^{-7}$ H/m is the permeability of free space, $\omega = 2\pi f$ the angular frequency, M the electrical moment of the stroke, and α and β two wave form parameters related to the channel length and the channel diameter of the stroke (VOLLAND, 1982).

The averaging process for GDD and SAR assures that the stroke parameters M, α, and β are already mean values for a particular thunderstorm. It is assumed that they do not change very much from one thunderstorm to the next. Combinating eqs. (3) to (7), it follows that $\overline{\text{GDD}}$ and $\overline{\text{SAR}}$ are linear functions of the distance ρ from the source:

$$\overline{\text{SAR}} \simeq a_1 + b_1\rho \; ; \quad \overline{\text{GDD}} \simeq a_2 + b_2\rho . \tag{8}$$

The parameters a_1 and a_2 contain primarily the average source properties via the mean parameters α and β in eq. (7). Note, however, that neither $\overline{\text{SAR}}$ nor $\overline{\text{GDD}}$ depend on the electrical moment M of a sferic. At the output of the receiver, the receiver constants must be added so that the measured constants a_1 and a_2 do not describe the true source terms.

The parameters b_1 and b_2 contain the wave guide characteristics via the factors A and B in eq. (5). These factors depend on frequency, azimuth, and time.

After elimination of ρ in eq. (8), one obtains a linear relationship between $\overline{\text{SAR}}$ and $\overline{\text{GDD}}$:

$$\overline{\text{SAR}} = C_1 + C_2\overline{\text{GDD}} , \tag{9}$$

where

$$a_1 = C_1(\phi) + C_2(\phi)a_2 \quad \text{and} \quad C_2(\phi) = b_1/b_2 \, . \tag{10}$$

As an example, Fig. 4 shows $\overline{\text{GDD}}$ *vs.* $\overline{\text{SAR}}$ for the data obtained at the Pretoria station during January 1984, for the time interval 1200 to 1600 GMT and for the two azimuthal sectors 346°—15° and 286°—315°. Numbers indicate the multiplying of each data point. In spite of the scatter, the linear relationship of eq. (9) is clearly supported by the data. The dash-dotted lines in Fig. 4 are the regression lines. Their slopes depend on the azimuthal angle ϕ. However, all regression lines should intersect at the common point (a_1, a_2) which is the origin of the graph $(\overline{\text{SAR}} - a_1, \overline{\text{GDD}} - a_2) = (b_1\rho, b_2\rho)$. In this specific case, we find $a_1 = -12$ db; $a_2 = -35$ μs, and

$$b_1/b_2 \simeq 0.18 + 0.03 \sin \phi \, . \tag{11}$$

One has to repeat this kind of analysis for other times of day and season for each station.

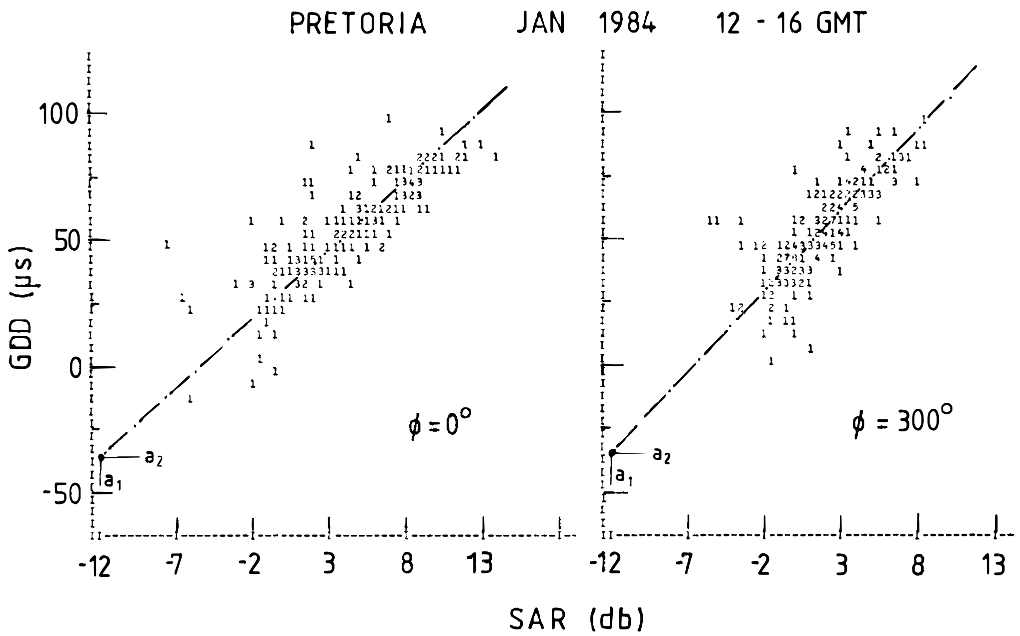

Fig. 4. Plots of GDD-values vs. SAR-values during sunlit hours (1200 to 1600 GMT) in January 1984, at the Pretoria station for the two azimuthal sectors 346°–15° (left) and 286°–315° (right). The dash-dotted lines are the regression lines. (a_1, a_2) is the point of intersection of both regression lines.

The scattering about the regression line in Fig. 4 is due to:

(a) Man-made noise; this corresponds to singular points far away from the regression line. It can be eliminated by allowing only a certain deviation from the regression line.

(b) Day-to-day variations of the ionospheric D layer; the effect of such variations is relatively small during day time hours but may be serious during night time conditions.

(c) Changes in the average properties of lightning strokes from one thunderstorm to the next due to changing meteorological conditions; if, for instance, the average channel length of the strokes varies by 20%, the variation would cause the scatter of

$\overline{SAR}$ and $\overline{GDD}$ observed in Fig. 4.
It is not possible to eliminate the scatter due to points (b) and (c). This scatter gives rise to errors in the calculated distance. On a map, a long living stationary source appears therefore as a cluster of points elongated in the direction of arrival.

4. Determination of the Distance of the Sources

There remains the determination of the coefficients b_1 and b_2 from which one can derive the distance of the sources. We determined these quantities by means of triangulation using strong sources observed simultaneously at Pretoria and at the von-Neumayer station. In addition, rain fall records prepared by the German Oceanographic Weather Agency (Deutsches Seewetteramt) in Hamburg were used. As an example, Fig. 5 shows the distribution of thunderstorms observed at the von-Neumayer station. Each point corresponds to the location of a thunderstorm as observed during each 20-min measurement cycle in June 1983. The fat points indicate locations where precipitation of 100 to 300 mm was measured during June 1983. The fat open circles indicate places with precipitation rates of 300 to 500 mm.

Two strong source areas can be identified: one source off the east coast of South America between 18° and 37° latitude, and a second source in the Indian Ocean southeast of South Africa in the neighborhood of Prince-Edward-Island. Both sources

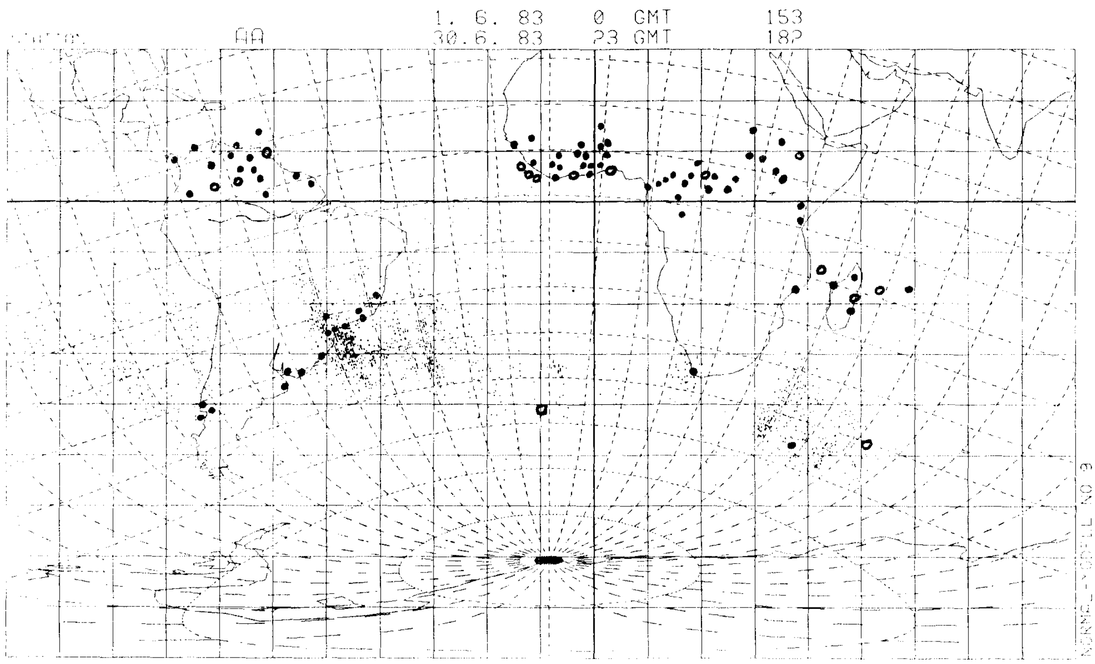

Fig. 5. Thunderstorm distribution map for June 1983, as derived from data recorded at the von-Neumayer station. Each point represents the location of one or more thunderstorm centers observed during the measurement cycle of 20 min. Dashed curves are isolines of distance (unit: 1000 km) and azimuth (unit: 10°). Fat points indicate stations with rain fall records of 100 to 300 mm during June 1983. Fat open circles indicate stations with rain fall records between 300 and 500 mm during the same month (prepared by the German Oceanographic Weather Agency (Deutsches Seewetteramt) in Hamburg).

can also be seen on the sferic records of Pretoria and on the precipitation map. Although rain fall rates are only loosely related to thunderstorm activity, they give a fair estimate of thunderstorm rates, at least on a statistical basis.

Using the known distances of these sources, the coefficients b_1 and b_2 are derived for the von-Neumayer station as function of time of day and of azimuth. Surprisingly, no significant daily variation is observed in the data. Their azimuthal dependence during June is given by

$$b_1 \simeq 5.4 + 1.4 \sin(\phi - D); \quad b_2 \simeq 31.4\ , \tag{12}$$

b_1 has the dimension (db/Mm); b_2 has the dimension (μs/Mm) with 1 Mm = 1000 km. $D = -22°$ is the geomagnetic declination at the von-Neumayer station.

Remarkable in eq. (12) is the near absence of an azimuthal dependence in b_2 and a relatively small ϕ-dependence in b_1. At mid-latitudes, this azimuthal variation is much larger (see Fig. 1 of VOLLAND *et al.*, 1983). This indicates a strong reduction of the anisotropic behavior of the atmospheric wave guide with respect to VLF waves at high southern latitudes as compared with mid-latitude conditions.

If we compare the numbers of b_1 and b_2 in eq. (12) with theoretical calculations of north-to-south propagation based on mid-latitude conditions (SCHÄFER and VOLLAND, 1982), we deduce an ionospheric D layer at southern high latitudes similar to night time conditions at mid-latitudes during winter with a virtual reflection height of about $z_0 \simeq 82$ km and an electron density profile of

$$N \simeq N_0 \exp[\lambda(z - z_0)]\ , \tag{13}$$

where $N_0 \simeq 3 \times 10^8$ m^{-3} and $\lambda \simeq 0.4$ km^{-1} .

The rather constant night time behavior of the ionospheric D layer results probably from electron precipitation of magnetospheric origin into the area of the geomagnetic South Atlantic anomaly (TORR *et al.*, 1975; BENBROOK *et al.*, 1983).

5. Conclusion

VLF sferics data from the German antarctic von-Neumayer station are available from January 18 to July 9, 1983. In this paper, we have analyzed the data of June 1983, in order to determine the propagation characteristics of the atmospheric wave guide between the earth and the ionospheric D layer during this time of the year. A complete data evaluation will be published elsewhere.

Acknowledgments

We are very grateful to all people at the von-Neumayer station and at the Alfred-Wegener-Institut für Polarforschung who contributed to the successful operation of the VLFAA station in the Antarctic. Our special thanks are due to Klaus WALLNER and Arno BRODSCHOLL who were in charge of the experiment at the von-Neumayer station. The tragic death of Klaus WALLNER at the end of this mission is deeply regretted.

References

BENBROOK, J. R., BERING III, E. A., LEVERENZ, H., ROEDER, J. L. and SHELDON, W. R. (1983): Quiettime electron precipitation at $L=4$ in the South Atlantic anomaly. J. Geophys. Res., **88**, 189–199.

HARTH, W. (1982): Theory of low frequency wave propagation. Handbook of Atmospherics, Vol. 2, ed. by H. VOLLAND. Boca Raton, CRC Press, 133–202.

SCHÄFER, J. and VOLLAND, H. (1982): VLF-atmospherics as a tool for probing VLF propagation conditions. AGARD Conf. Proc., **305**, 6-1.

SPAULDING, A. D. (1982): Atmospheric noise and its effects on communication system performance. Handbook of Atmospherics, Vol. 1, ed. by H. VOLLAND. Boca Raton, CRC Press, 289–328.

TORR, D. G., TORR, M. R. and WALKER, J. C. G. (1975): Particle precipitation in the South Atlantic anomaly. Planet. Space Sci., **23**, 15–26.

VOLLAND, H. (1982): Low frequency radio noise. Handbook of Atmospherics, Vol. 1, ed by H. VOLLAND. Boca Raton, CRC Press, 179–250.

VOLLAND, H., SCHÄFER, J., INGMANN, P., HARTH, W., HEYDT, G., ERIKSSON, A. J. and MANES, A. (1983): Registration of thunderstorm centers by automatic atmospherics stations. J. Geophys. Res., **88**, 1503–1518.

(Received January 26, 1985; Revised manuscript received July 22, 1985)